

Automatic quality control of telemetric rain gauge data providing quantitative quality information (RainGaugeQC)

Katarzyna Ośródk¹, Irena Otop², Jan Szturc¹

¹Centre of Meteorological Modelling, Institute of Meteorology and Water Management – National Research Institute, PL 01-673 Warszawa, Podleśna 61, Poland

²Research and Development Centre, Institute of Meteorology and Water Management – National Research Institute, PL 01-673 Warszawa, Podleśna 61, Poland

Correspondence to: Jan Szturc (jan.szturc@imgw.pl)

Abstract. The RainGaugeQC scheme described in this paper is intended for real-time quality control of telemetric rain gauge data. It consists of several checks: detection of exceedance of the natural limit and climate-based threshold, and checking of the conformity of rain gauge and radar observations, the consistency of time series from heated and unheated sensors, and the spatial consistency of adjacent gauges. The proposed approach is focused on assessing the reliability of individual rain gauge observations. A quantitative indicator of reliability, called the quality index (QI), describes the quality of each measurement as a number in the range from 0.0 (completely unreliable measurement) to 1.0 (perfect measurement). The QI of a measurement which fails any check is lowered, and only a measurement very likely to be erroneous is replaced with a “no data” value. The performance of this scheme has been evaluated by analysing the spatial distribution of the precipitation field and comparing it with precipitation observations and estimates provided by other techniques. The effectiveness of the RainGaugeQC scheme was also analysed in terms of the statistics of QI reduction. The quality information provided is very useful in further applications of rain gauge data. The scheme is used operationally by the Polish national meteorological and hydrological service (Institute of Meteorology and Water Management – National Research Institute).

1 Introduction

The accuracy of telemetric rain gauge data is vital both for scientific research and for real-time modelling. Reliable precipitation measurements with high temporal and spatial resolution are essential input data for numerous operational applications in meteorology and hydrology, such as quantitative precipitation estimation (QPE), nowcasting, real-time initial conditions for numerical weather prediction, hydrological modelling, etc. Incorrect values may affect the results of these applications; this applies especially to unreasonably high or false zero precipitation values.

In recent decades, the number of automated weather station networks providing measurements with high temporal resolutions (e.g. 1-, 5-, or 10-minute) has rapidly increased. Consequently, procedures for data quality control (QC) have developed from manual or semiautomatic to fully automatic checks that provide relevant quality information, such as quality flags or quality indices (Lewis et al., 2021). However, in the case of precipitation, the effectiveness of automatic quality control methods has been proven to be much lower than in the case of other meteorological parameters (You et al., 2007). The key issue is the spatiotemporal variability of the precipitation field, which can be very intermittent and small-scale, depends strongly on the type of precipitation (e.g. convective or frontal), and also depends on topographic variables in mountainous areas with complex terrain (Scherrer et al., 2011).

This paper presents the RainGaugeQC software, which is a package of automatic QC procedures, developed at the Institute of Meteorology and Water Management – National Research Institute (IMGW), which operates the Polish national meteorological and hydrological service. The scheme focuses on telemetric rain gauge measurements, and is designed to identify erroneous or suspicious data and to assign a quality index (QI) to the individual measurements. The RainGaugeQC

39 was designed specifically for quality control of sub-hourly rain gauge data. This is a particularly challenging task because of
40 the higher spatial variability and lower spatial consistency of such data (Villalobos Herrera et al., 2022).

41 **1.1 Sources of errors in rain gauge data**

42 Ground rain gauge measurements, like other observations, are affected by different types of errors, usually classified as
43 random, systematic and gross errors. Random errors vary in an unpredictable manner, while systematic errors remain constant
44 or vary in a predictable way, and can often be reduced. Gross errors are characterised by rare occurrence and large magnitude
45 (WMO-No. 488, 2017).

46 Problems relating to the accuracy of precipitation measurement have been well documented (e.g. Sevruk, 1996; Habib
47 et al., 2001; Golz et al., 2005; Sieck et al., 2007; Sevruk et al., 2009). The magnitude of measurement errors depends on many
48 factors, including weather conditions at the collector, the location of the rain gauge, and the gauge type. The most significant
49 measurement errors are related to wind (Sevruk et al., 2009; Rasmussen et al., 2012; Martinaitis et al., 2015). Wind-induced
50 losses mainly depend on wind speed and turbulence, as well as the type of precipitation (e.g. rain, mixed snow and rain, or
51 snow). The measurement error is usually greater for solid than for liquid precipitation (WMO-No. 8, 2018). Because of slow
52 falling, snow hydrometers are more susceptible to deflection by wind-induced turbulence around the gauge, making snowfall
53 measurements prone to large systematic errors (Rasmussen et al., 2012). In windy conditions, the underestimation of snowfall
54 accumulation frequently ranges from 20% to 50% or even higher, and additionally depends on other variables, such as exposure
55 and the type of rain gauge (Rasmussen et al., 2012; Buisán et al., 2017; Grossi et al., 2017). Other systematic error sources are
56 related to physical processes, such as evaporation from a bucket, wetting, and splashing. All such errors are typically referred
57 to as catching losses.

58 Additional difficulties occur in winter precipitation measurements as a result of snow collecting on the gauge or snow
59 accumulating within wind shields, either of which can completely or partially block the gauge orifice (Goodison et al., 1998;
60 Rasmussen et al., 2012; Martinaitis et al., 2015; Kochendorfer et al., 2020). In consequence, Martinaitis et al. (2015) identified
61 a secondary but important impact from gauges that had become partially or completely stuck during winter precipitation events.
62 Thawing due to increased surface ambient temperatures resulted in gauges reporting false non-zero precipitation after having
63 collected solid precipitation. These impacts became increasingly complex when rainfall occurred simultaneously with the
64 thawing of accumulated solid precipitation.

65 Moreover, the accuracy of precipitation measurements may be affected by improper exposure of the gauge, site altitude,
66 shielding or obstacles (e.g. trees, buildings) near the rain gauge, the impact of topographic variables in complex areas, and the
67 seeder–feeder effect (when precipitation from an upper-level cloud falls through a lower-level orographic stratus cloud capping
68 a small mountain) (Førland et al., 1996; Sevruk and Nevenic, 1998).

69 Additionally, mechanical problems specific to each type of rain gauge influence the accuracy of precipitation
70 measurements. Tipping bucket rain gauges are subject to random errors related to partial or total blockages of the mechanism
71 due to accumulated mineral or biological particulates: dust, insects, blown grass, etc. (Sevruk, 1996; Upton and Rahimi, 2003).
72 In consequence, even partial clogging of the gauge can result in erroneous estimates of the intensity and duration of rainfall.
73 Another specific problem with tipping bucket rain gauges relates to high-frequency bucket tips (double tips), which lead to the
74 recording of spurious high rainfall intensities, while on the other hand very slow tips (i.e. a limited tipping rate) may result in
75 misleading underestimates of rain rates (Upton and Rahimi, 2003; Shedekar et al., 2016).

76 In the case of weighing gauges, the most relevant sampling errors are related to the response time of the measurement
77 system and the consequent systematic delay in assessing the exact weight of the accumulated precipitation in the container,
78 especially in the case of high resolution (e.g. a 1-minute time resolution). Sampling errors may also affect the measurement of
79 low-intensity rain (Colli et al., 2013).

80 Electronic weighing precipitation gauges are less susceptible to evaporation losses than tipping bucket gauges and have
81 better accuracy in assessing the beginning of snowfall events. A heated tipping bucket gauge starts recording with a delay due
82 to the time needed to melt the snow and fill the first tip, and measures less precipitation due to heating-related losses (Savina
83 et al., 2012).

84 Furthermore, precipitation measurements may be affected by gross errors, mainly caused by the malfunctioning of
85 measurement devices, or occurring during data transmission.

86 **1.2 Approaches to quality control of rain gauge data**

87 Quality control is a vital part of data processing in order to achieve a certain standard for international data exchange. The
88 World Meteorological Organisation (WMO) recommends initially to perform real-time basic QC of raw data at sensor level,
89 then near-real-time QC, and finally non-real-time extended QC (semi-automatic) at the headquarters (WMO-No. 488, 2017).
90 Performing QC at various stages of data processing makes it possible to identify the majority of errors in the dataset.

91 Generally speaking, some precipitation data QC checks consider each single observation separately (Upton and Rahimi,
92 2003; Taylor and Loescher, 2013; Blenkinsop et al., 2017), whereas more complex ones also take into account data from
93 neighbouring stations (Steinacker et al., 2011; Scherrer et al., 2011) or multi-source data, such as weather radar data (Yeung
94 al., 2014; Baserud et al., 2020) and output from a numerical weather prediction model (Qi et al., 2016). Recently, due to the
95 increased utilisation of crowdsourced observations, specific QC methods applicable for this type of precipitation data have
96 been developed (de Vos et al., 2019; Bárdossy et al., 2021; Niu et al., 2021).

97 For assessing the reliability of observations, several approaches are adopted. In practice, various measures of the quality
98 of precipitation data are used. They indicate the reliability of individual sensors resulting from measurement precision, which
99 is strongly conditioned by construction and technology (Førland et al., 1996), location, current meteorological conditions
100 (wind, temperature), etc. Often, flags describing the quality of the data are used qualitatively; for example, the WMO
101 recommends a scheme of five quality flags, defined as good, inconsistent, doubtful, erroneous, and missing (WMO-No. 488,
102 2017, p. 201).

103 In the simple approach to QC outputs, the only possible result is the acceptance or rejection of particular observations.
104 An observation that passes all of the checks is flagged as correct. If an observation fails a check, it is flagged as incorrect and
105 does not undergo the remaining checks (Baserud et al., 2020); however, it is possible to retrieve information on which test was
106 failed for each observation. Some QC schemes integrate the results of individual QC checks to generate a final flag for each
107 observation. In this case an adjustment test or specially designed rule base is applied to minimise the number of correct
108 observations that are flagged as “erroneous”. For example, if an observation failed a climate-based range test but passed the
109 spatial check, then an adjustment test may reduce the severity of the flag obtained from the climate-based range check (Fiebrich
110 et al., 2010; Lewis et al., 2018; 2021).

111 In another approach, after failing specific checks the measured values are not removed, but corrected. Such a method
112 may be used to replace suspicious data with values obtained from interpolation data from neighbouring stations (Michelson,
113 2004), but it does not provide any additional information. Also, the use of data from other measurement systems is not a
114 satisfactory solution, as these data are generally inconsistent with each other due to their different spatial distributions.
115 Generally, the correction of measured values can give unreliable results due to the high level of arbitrariness.

116 Recently, machine learning using artificial neural networks has been employed as a tool for automated quality control
117 as well as for the correction of errors and reconstruction of missing values in precipitation data (Moslemi and Joksimovic,
118 2018).

119 Quantitative indicators describing the quality of the observations can also be used, most often as a quality index
120 (QI) ranging from 0.0 (completely unreliable measurement) to 1.0 (perfect measurement) (Einfalt et al., 2010; Szturc et al.,
121 2022). This approach is adopted in the QC scheme described in this paper. In the developed RainGaugeQC scheme, the quality

122 of uncertain measurements is lowered and only measurements very likely to be erroneous are removed – they are replaced
123 with “no data” values. The advantage of this approach is that the quality information can be very useful in further applications.
124 For example, it is employed in quality-based spatial interpolation of rain gauge data and in merging observations from different
125 measurement techniques (e.g. Jurczyk et al., 2020). It seems optimal to take into account quantitative information about the
126 quality of individual measurements in such a way that the more uncertain data are assigned a lower weight than more reliable
127 data.

128 1.3 Structure of the paper

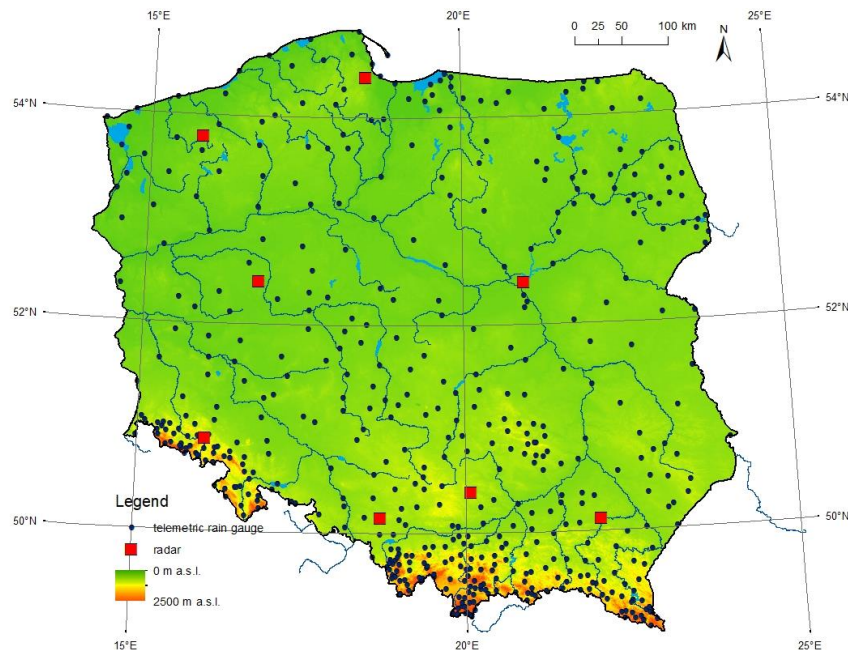
129 The paper is structured as follows. After section 1, section 2 briefly describes the rain gauge data on which the RainGaugeQC
130 scheme proposed in the paper was developed and calibrated, as well as the radar data used as auxiliary data in this scheme. In
131 section 3, the checks that constitute the RainGaugeQC system are presented (their detailed descriptions are included in the
132 appendices). Section 4 presents and discusses specific examples of the scheme’s performance and a general analysis of its
133 operation. The article ends with a list of conclusions resulting from the operational use of the RainGaugeQC scheme at IMGW
134 (section 5).

135 2 Data sources

136 2.1 Rain station network in Poland

137 The Polish national meteorological and hydrological service, provided by IMGW, operates a nationwide meteorological
138 telemetric network which consists of 503 rain stations equipped mainly with tipping bucket sensors (Fig. 1). At the synoptic
139 stations, SEBA Hydrometrie (<https://www.seba-hydrometrie.com/>) RG-50 devices are installed, whereas precipitation stations
140 use mainly the Met One Instruments (<https://metone.com/>) 60030 and 60030H devices (unheated and heated, respectively).
141 Telemetric precipitation measurements are available with a 10-minute time resolution: all year round for heated sensors, and
142 in the warm part of the year – from April to October – for unheated ones.

143
144



145
146
147

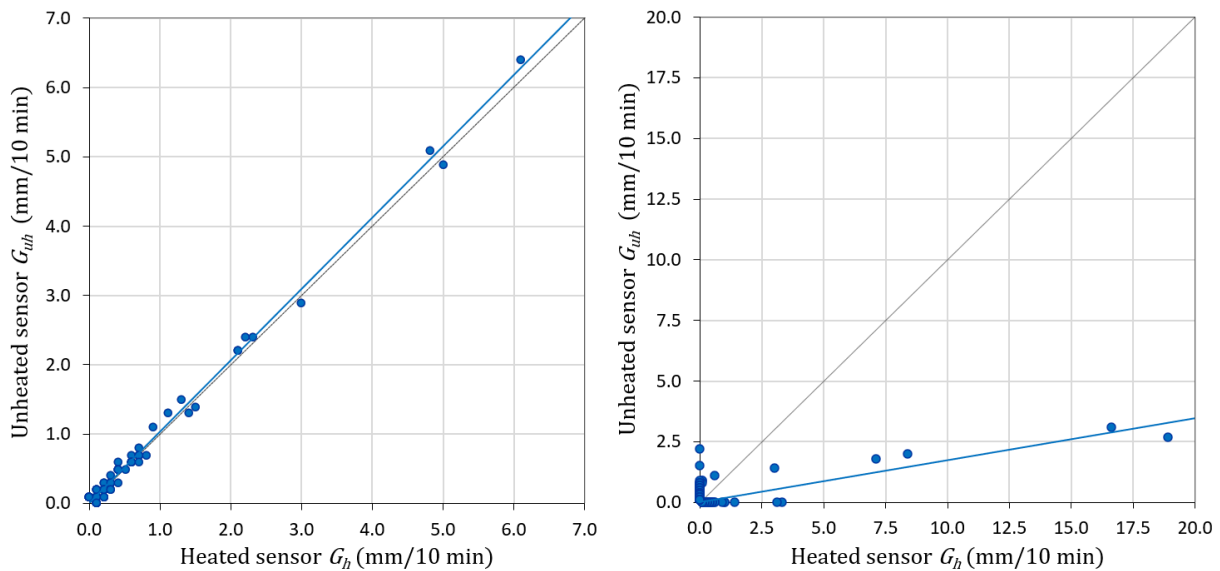
Figure 1: Networks of telemetric rain stations and weather radars in Poland.

148 The reliability of individual rain gauge depends on the type of the gauge and its location, and changes with time. The
149 network's tipping bucket devices often malfunction, and moreover these sensors lower the precipitation values by an average
150 of about 8–20% (Urban and Strug, 2021).

151 Fig. 2 shows the relationships between measurements of 10-minute precipitation accumulations from unheated and
152 heated sensors on two sample rain stations: in Dzierżoniów, located in the foothills area, during July 2021 (left), and in Nowa
153 Wieś Podgórna, located in the lowland Wielkopolska (Greater Poland) region in central Poland, during June 2021 (right). Both
154 stations are equipped with two tipping bucket sensors. The following denotations are introduced for the precipitation values
155 they measure: G_h is the 10-min precipitation amount observed by the heated sensor, and G_{uh} is the analogical value observed
156 by the unheated one. The correlation coefficient calculated for pairs of values in which at least one is different from zero is
157 extremely high for Dzierżoniów, being equal to 0.997 (Fig. 2a), while for Nowa Wieś Podgórna it is only 0.694 (Fig. 2b), a
158 fairly low result caused by very large differences between the values measured simultaneously by the two sensors at the same
159 location. The reason for such low correlation may be that tipping bucket gauges are susceptible to frequent sensor failures.

160 Generally, the left graph of Fig. 2 corresponds to a well-functioning rain station, and the right graph corresponds to a
161 rain station with one or both sensors not functioning correctly, therefore they require effective quality control. It is shown in
162 section 4.3, concerning an example case study, how the quality control scheme presented in this paper worked on these
163 obviously incorrect measurements.

164



165



166

167

168 **Figure 2: Relationships between observations of 10-minute precipitation accumulations measured with tipping bucket rain stations**
169 **equipped with two sensors – unheated and heated – in Dzierżoniów during July 2021 (left) and in Nowa Wieś Podgórna during June**
170 **2021 (right). The blue lines mark the trends of these relationships. The data from 3 rain stations showed at the bottom map are**
171 **discussed in the examples.**

172 2.2 Weather radar data

173 Weather radar data are employed in the RainGaugeQC scheme as auxiliary data to verify rain gauge observations. They are
174 generated by the Polish radar network POLRAD, which consists of eight C-band Doppler radars from Leonardo Germany
175 GmbH (formerly Gematronik and Selex) (Szturc et al., 2018). Three of them are dual-polarisation radars, and work is currently

176 underway on upgrading all the radars, including dual polarization functionality. Three- and two-dimensional radar products
 177 are generated by Rainbow 5 software every 10 min, with a 1 km spatial resolution within a 215 km range. The Marshall–
 178 Palmer formula is used to transform the reflectivity values measured by radar into the precipitation rate, this being the most
 179 common form of such a relationship (Neuper and Ehret, 2019). The data are quality controlled by the dedicated RADVOL-
 180 QC system developed at IMGW (Ośródka et al., 2014; Ośródka and Szturc, 2022). The system also generates quality fields,
 181 $QI(R)$, based on analyses of particular errors disturbing radar data.

182 2.3. Other data

183 In addition, the fields of the following precipitation estimates were used for the case studies:

- 184 – satellite precipitation fields determined from various NWC-SAF (Satellite Application Facilities on Support to
 185 Nowcasting and Very Short Range Forecasting) products based on Meteosat data (Jurczyk et al., 2020),
- 186 – QPE fields produced by the RainGRS system, which operationally combines precipitation data from rain gauges,
 187 weather radar and meteorological satellites, based on conditional merging and additionally taking quality information
 188 into account (Jurczyk et al., 2020).

189 3 General description of the developed quality control scheme

190 3.1 Set of RainGaugeQC algorithms

191 A shortened version of the description of the algorithms used in the scheme was presented in works by Otop et al. (2018) and
 192 Jurczyk et al. (2020). This section and the related appendices provide a full description of the developed algorithms. All
 193 parameters defined here were optimised for 10-minute precipitation accumulations (mm/10 min).

194
 195 **Table 1. List of sequential checks for precipitation QC.**

ID	Abbreviation	Name	Main approach	Result of the check
1	GEC	Gross Error Check	Detection of exceedance of the natural limit	Removal of incorrect values
2	RC	Range Check	Detection of exceedance of climate-based threshold at an individual gauge	QI reduction for suspiciously high precipitation value
3	RCC	Radar Conformity Check	Checking of the conformity of rain gauge and radar observations	Removal of false “no precipitation” data. For false precipitation reports, QI reduction depending on $SF(G_h, G_{uh})$ and location
4	TCC	Temporal Consistency Check	Checking of the consistency of time series from heated and unheated sensors	QI reduction for inconsistent sensors
5	SCC	Spatial Consistency Check	Checking of the spatial consistency of adjacent gauges	QI reduction for outliers depending on the inconsistency level

196
 197 The rain gauge quality control procedure developed at IMGW consists of several checks (Table 1). Firstly, simple
 198 plausibility tests – the gross error check and range check – are performed on a single measurement. Then more complex checks
 199 are performed, using data from both measurement sensors at the site and data from weather radars.

200 Before the checks, each sensor is assigned the perfect QI value (1.0). In case of failure of a particular check, the QI
 201 value is decreased by a specified value. If the final QI value (after all of the checks) is very weak (≤ 0.0), the sensor is
 202 considered useless and the measurement value is replaced with “no data”.

203 The sensor which obtained a higher final quality index is used for further applications, but if both sensors are of the
 204 same quality, then the heated sensor is taken.

205 3.2 Similarity function (SF)

206 It is useful to introduce a tool to check the similarity of two sums of precipitation. For this purpose a similarity function (SF)
 207 has been proposed and is used in some of the checks. The function $SF(G_h, G_{uh})$, comparing precipitation data from two sensors

208 G_h and G_{uh} (heated and unheated) installed at the same rain station G in order to check whether the measured values are
 209 consistent, is defined as follows:

210 If ($G_h < 1.0$ mm or $G_{uh} < 1.0$ mm), then

211 if ($|G_h - G_{uh}| < 1.0$ mm), then $SF(G_h, G_{uh}) = \text{“true”}$ (1)

212 else $SF(G_h, G_{uh}) = \text{“false”}$

213 whereas:

214 If ($G_h \geq 1.0$ mm and $G_{uh} \geq 1.0$ mm), then

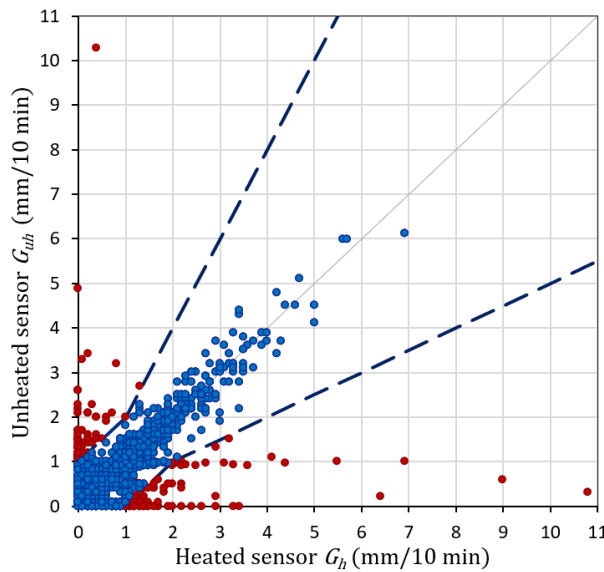
215 if ($0.5 < \frac{G_h}{G_{uh}} < 2.0$ or $|G_h - G_{uh}| < 1.0$ mm), then $SF(G_h, G_{uh}) = \text{“true”}$ (2)

216 else $SF(G_h, G_{uh}) = \text{“false”}$

217 In the above formulae, precipitation units are given in “mm”, but they may refer to different accumulation periods, for
 218 example, mm per 10 minutes (mm/10 min) or 1 hour.

219 The result of the use of SF to assess the similarity of measurements between two sensors (heated and unheated) in rain
 220 stations is presented in Fig 3. The graph shows example data for one day, 22 May 2019, obtained from all measuring stations.
 221 It is indicated which measurements from the two sensors are shown by the SF function to be similar (marked blue) and which
 222 are not similar (marked brown). The two blue dashed lines delimit the area in which the values measured by the unheated and
 223 heated sensors are similar according to the SF function.

224



225

226

227 **Figure 3: Precipitation data from G_{uh} and G_h sensors that are similar (blue) and not similar (brown). The similarity of the**
 228 **measurements from all rain stations on 22 May 2019 was determined using the similarity function SF. The two dashed lines delimit**
 229 **the area in which the measurements are considered similar.**

230 **3.3 Gross Error Check (GEC)**

231 GEC is a preliminary check to identify gross errors which have a strong effect on the further analyses. These errors are mainly
 232 caused by the malfunctioning of measurement devices or by mistakes occurring during data transmission or processing
 233 (Steinacker et al., 2011). GEC examines whether the rain gauge measurement is within the physically acceptable range limits:
 234 not less than 0 mm and not above 56 mm/10 min (i.e. 51 dBZ). The upper limit was determined on the basis of a formula

235 developed to estimate the maximum reliable precipitation for various durations in Poland (Burszta-Adamiak et al., 2019). A
236 measurement that fails the check is rejected from further processing.

237 **3.4 Range Check (RC)**

238 RC verifies a single measurement against a threshold value, which is based on local climatological data with respect to seasonal
239 variation of observations in the specific location of the rain station. This test identifies data as implausible when they exceed
240 the expected maximum value, that is, the threshold empirically estimated from long-term climatological data. It is essential to
241 ensure reliable values of the threshold, because, for example, too low a threshold may cause extreme values of precipitation to
242 fail the test (Taylor and Loescher, 2013). Therefore, Fiebrich et al. (2010) recommend developing regionally specific
243 thresholds for the test. In the proposed QC procedure, the thresholds were defined as 10-minute precipitation values with a 1%
244 probability of being exceeded, determined separately for warm and cold seasons. These values were calculated for each
245 telemetric station, based on the statistical distribution of 10-minute accumulations in a 30-year time series (1986-2015). In the
246 case that the examined measurement exceeds the relevant threshold value, it is treated as suspicious and its QI is reduced by
247 0.25.

248 **3.5 Radar Conformity Check (RCC)**

249 RCC is performed to identify false precipitation – false zero and false gauge-reported precipitation measurements – on the
250 basis of radar data, which quite reliably indicate the spatial distribution of precipitation. RCC compares each gauge observation
251 lower than 0.2 mm/10 min with radar observations at the gauge location and its surrounding of 3 pixels x 3 pixels (the pixel
252 size is 1 km x 1 km). If the radar data for the vicinity of the station are above a predefined threshold, then a “no precipitation”
253 result measured by the sensor is assumed to be false and the QI is reduced to 0.0.

254 On the other hand, the RCC compares every sensor observation $G > 0$ mm/10 min with radar observations at the gauge
255 location and its neighbouring of 3 pixels x 3 pixels. If the radar data is of a quality $QI(R)$ above a predefined threshold and
256 indicates “no precipitation” (0 mm), then the precipitation measured by the sensor is assumed to be false and the QI of that
257 observation is reduced. The reduction depends on whether data are available from one or two sensors, on their similarity, and
258 on the gauge location. The following regions based on altitude are distinguished: lowlands (areas below 300 m a.s.l.), foothills
259 (between 300 and 600 m a.s.l.), and mountainous (areas above 600 m a.s.l.).

260 For a detailed description of the RCC algorithm and the criteria for determining the reduction of QI , see Appendix 1.

261 **3.6 Temporal Consistency Check (TCC)**

262 This check, in the form described below, is possible only when two sensors are installed at each measuring station, most often
263 heated and unheated, as is currently the case in the IMGW network. If this is not the case, then a method commonly used in
264 quality control of various meteorological quantities is to check the time continuity of the measured values. For some types of
265 meteorological data the time consistency checks are efficient; however, in the case of precipitation data, this check would
266 eliminate not only all questionable data but also a large amount of true data, in particular extreme values, because of the high
267 variability of precipitation (WMO-No. 305, 1993, p. VI.21, VI.23).

268 The first step of this check is performed to detect a clogged sensor, which occurs if the same value is repeated over a
269 certain period of time. In this case, the sensor’s quality is reduced to 0.0.

270 In the next step, pairs of rain gauge sensors (G_h, G_{uh}) are tested for the existence of large differences between them.
271 This check requires measurements from both rain gauge sensors at the same location, and can thus be conducted only in the
272 warm half of the year, because only then two time series from the same station are available. In this procedure, if the number

273 of measurement pairs is sufficient, they are accumulated and their similarity is checked using the SF function (see section 3.2).
274 If the sums differ, the data from both sensors have failed the TCC check and their quality is reduced.

275 For a detailed description of the TCC algorithm see Appendix 2.

276 3.7 Spatial Consistency Check (SCC)

277 SCC is applied to identify outliers based on a comparison with neighbouring stations. Additionally, radar data are introduced
278 to assess the level of QI reduction for outliers.

279 There are several steps in the operational procedure for SCC. Firstly, the domain area is divided into basic subdomains
280 with a spatial resolution of 100 km x 100 km. For each subdomain, a set of percentiles of rain gauge data and the median
281 absolute deviation (MAD) are calculated.

282 The criterion for the spatial consistency of an individual sensor is implemented based on the index D , calculated using
283 the formula of Kondragunta and Shrestha (2006). This index is compared with the threshold values defined by set of percentiles
284 of the index D , making it possible to determine the different classes of outliers. The check is repeated for subdomains obtained
285 by making shifts of 25 km in all four directions. If the sensor value is identified as an outlier in the basic subdomain and in the
286 shifted subdomains, the sensor is detected as an outlier and a further procedure is applied to assess the relevant quality
287 reduction.

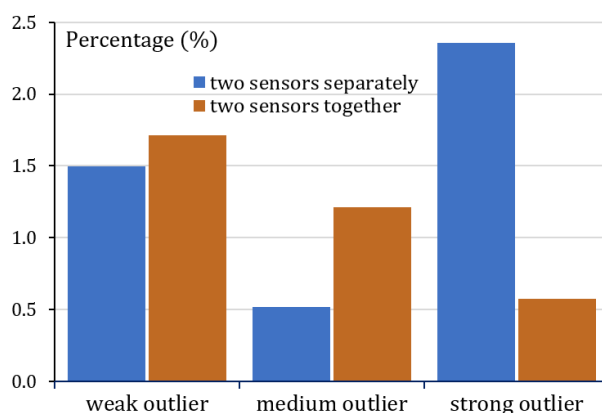
288 For each detected outlier, two criteria are checked: (i) if data from both sensors are available for a given rain gauge and
289 they are similar, i.e. $SF(G_h, G_{uh}) = \text{“true”}$, and (ii) if the data passed the TCC test. If both criteria are met, then the QI for the
290 sensor is not reduced. Otherwise, for additional verification, radar data in a grid of 5 pixels x 5 pixels around the gauge location
291 are considered if they are of good quality. In this case the reduction of the QI value depends on the class of the outlier (weak,
292 medium, or strong) and the magnitude of the disparity with the radar data (the limitation imposed on the magnitude of this
293 disparity has been determined empirically).

294 A detailed description of the SCC algorithm and the criteria for reduction of the QI value are given in Appendix 3.

295 The check may optionally analyse data from both sensors together or separately, and may include or not data from the
296 previous time step. It was investigated how these two settings influence the performance of the check.

297 Fig. 4 presents graphs showing the percentage of data with reduced QI values, as a result of analysing the spatial
298 conformity of data from two types of sensors (unheated and heated) separately or together. The obtained sample results
299 generally showed large variation; however, the numbers of strong outliers increased significantly (about 2.35% versus 0.6%)
300 when the two types of sensors were analysed separately – in that case the algorithm appears much less tolerant.

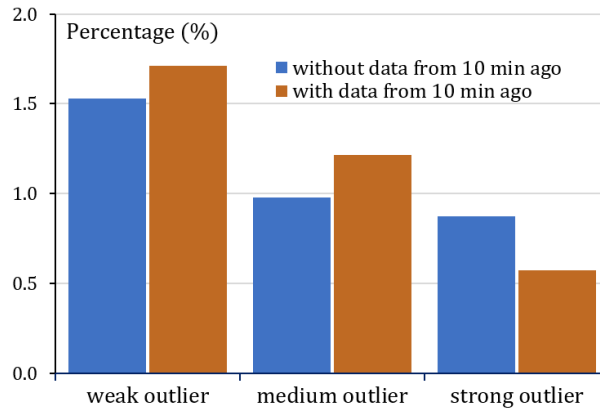
301



302
303
304
305

Figure 4: Percentage of classes of outliers (weak, medium, and strong) when analysing the data from two types of sensors (unheated and heated) separately (blue) or together (brown). Data from 22 May 2019.

306 If the algorithm takes into account data not only from the current time step, but also from 10 minutes ago (both sensors
 307 analysed together), then these numbers are slightly higher for weak and medium outliers and slightly lower for strong ones.
 308 The latter indicates that the inclusion of data from the previous time step makes the algorithm more tolerant.. The percentage
 309 of the data belonging to all classes of outliers together was slightly over 3% (Fig. 5), and for particular classes varies from
 310 about 1.5–1.7% for the weak to about 0.6–0.9% for the strong outliers.
 311



312
 313 **Figure 5: Percentage of classes of outliers (weak, medium, and strong) when analysing measurements from the given time only (blue)**
 314 **and also from the previous time step (brown). Data from two days: 20–21 June 2020.**
 315

316 In the RainGaugeQC scheme currently used by IMGW in real time, in the SCC check both types of sensors are analysed
 317 together, also taking account of the data from the previous time step.

318 3.8 Quality index of spatially distributed rain gauge data

319 In most applications of rain gauge data, spatial interpolation of the point data is required and this procedure can be carried out
 320 by any of a number of commonly known methods. However, it is not enough to spatially interpolate the QI values assigned to
 321 individual rain gauges. It is also necessary to take into account the fact that the uncertainty of the estimated field increases
 322 very quickly with increasing distance from the nearest rain gauge. Therefore, the quality field for the spatially distributed
 323 precipitation data depends on two factors: the QI point values for individual rain gauges (denoted by the QI with the index
 324 “ p ”) and a factor that depends linearly on the distance from the nearest rain gauge (with the index “ d ”).

325 The precipitation and QI point values from rain stations are spatially interpolated simultaneously by the same method
 326 using the same parameters, so in both cases there are the same contributions from the individual rain gauges. Hence the
 327 obtained quality field $QI(G_{int}(x, y))_p$ is completely consistent with precipitation field ($G_{int}(x, y)$). In the case of the operational
 328 scheme used by IMGW, ordinary kriging is applied, where the domain of 900 km x 800 km is divided into 16 subdomains of
 329 225 km x 200 km and interpolation is performed separately in each of them.

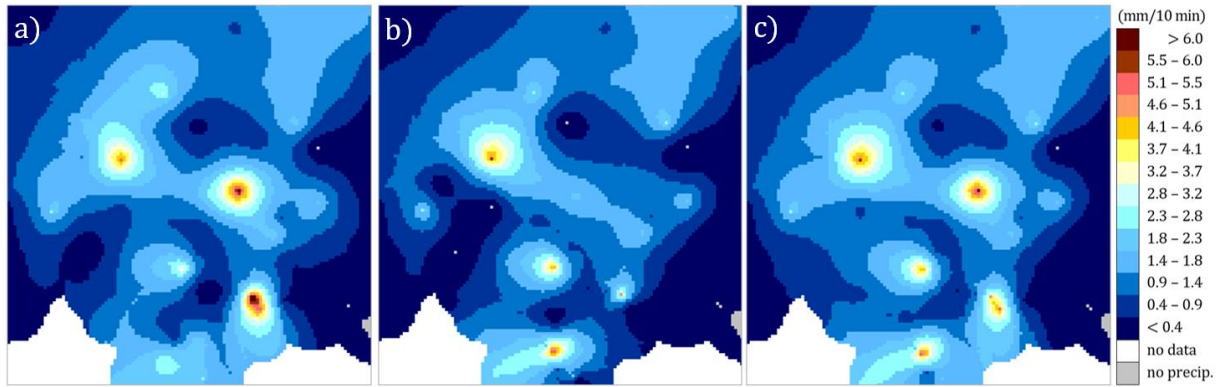
330 The factor related to the distance from the rain gauges $QI(G_{int}(x, y))_d$ takes into account the decrease in the quality of
 331 the rainfall field depending on the distance $d(x, y)$ to the nearest rain gauge. The distance factor for each pixel is calculated
 332 from the linear formula:

$$333 \quad QI(G_{int}(x, y))_d = \frac{d_{max} - d(x, y)}{d_{max}} \quad (3)$$

334 where d_{max} is the limit value of the distance to the nearest rain gauge, above which the quality at that pixel is assigned a value
 335 of zero (the adopted limit is 100 km).

336 The field of the final quality index for the rain gauge-based precipitation field is calculated from the product of the two
 337 above factors:

$$338 \quad QI(G_{int}(x, y)) = QI(G_{int}(x, y))_p \cdot QI(G_{int}(x, y))_d \quad (4)$$

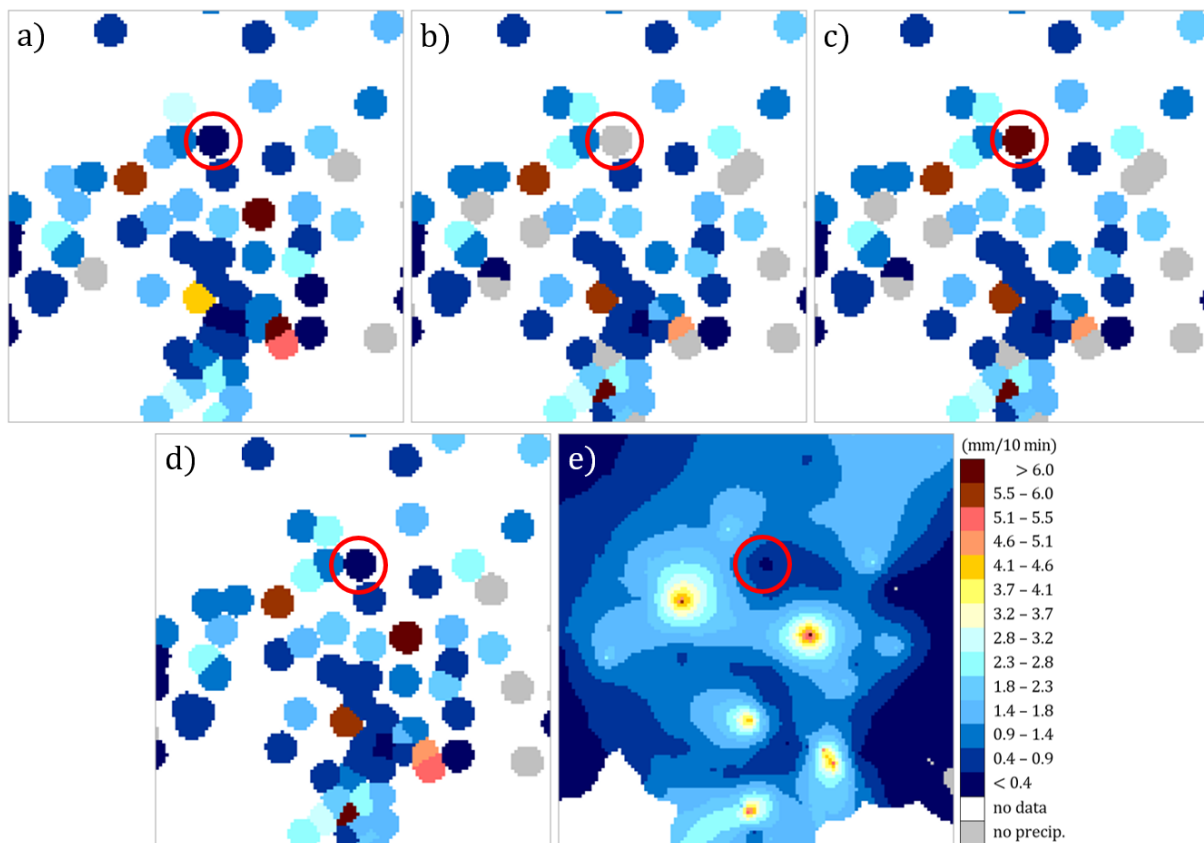


341
342
343 **Figure 6: Spatially interpolated rain station data obtained from: (a) unheated and (b) heated sensors, and (c) after quality control**
344 **(considered optimal). Data from 5 August 2021, 17:40 UTC, fragment from the Polish domain (240 km x 250 km).**

345 In the example presented in Fig. 6, it can be seen that the data from the two sensors can sometimes be significantly different.
346 In simpler solutions the final rainfall field can be generated by taking the mean or the higher values of the two sensors at the
347 same location, and both of these approaches can be justified depending on the final application of the data. The approach used
348 in the RainGaugeQC scheme makes it possible to choose the better value according to defined checks. Moreover, it enables to
349 apply that precipitation value along with the relevant QI value in quality-based interpolation algorithms which generate the
350 optimal rain gauge field.

351 4.2 Result of the performance of the QC scheme after the introduction of erroneous values

352 Fig. 7 illustrates the performance of the proposed QC scheme. If the rain gauge data are not subjected to QC algorithms, then
353 two alternative data sets can be considered: from unheated (Fig. 7a) and heated (Fig. 7b) sensors. The third diagram shows an
354 example of data disturbed with an artificial value of 10 mm/10 min at the heated sensor of the Siercza rain station (Fig. 7c),
355 which is marked with a red circle in all diagrams. Location of the Siercza rain station is shown in Fig. 2 (bottom).
356



357
358
359
360
361
362
363

Fig. 7. Example of the RainGaugeQC performance after the introduction of erroneous precipitation value: (a) original rain gauge data from unheated sensors (G_{uh}) (in all fields the Siercza rain station is marked with a red circle), (b) original data from heated sensors (G_h), (c) data from heated sensors disturbed with an artificial value at Siercza (10 mm/10 min), (d) rain gauge data after quality control, and (e) after spatial interpolation. Data from 5 August, 2021, 17:40 UTC, fragment from the Polish domain (240 km x 250 km).

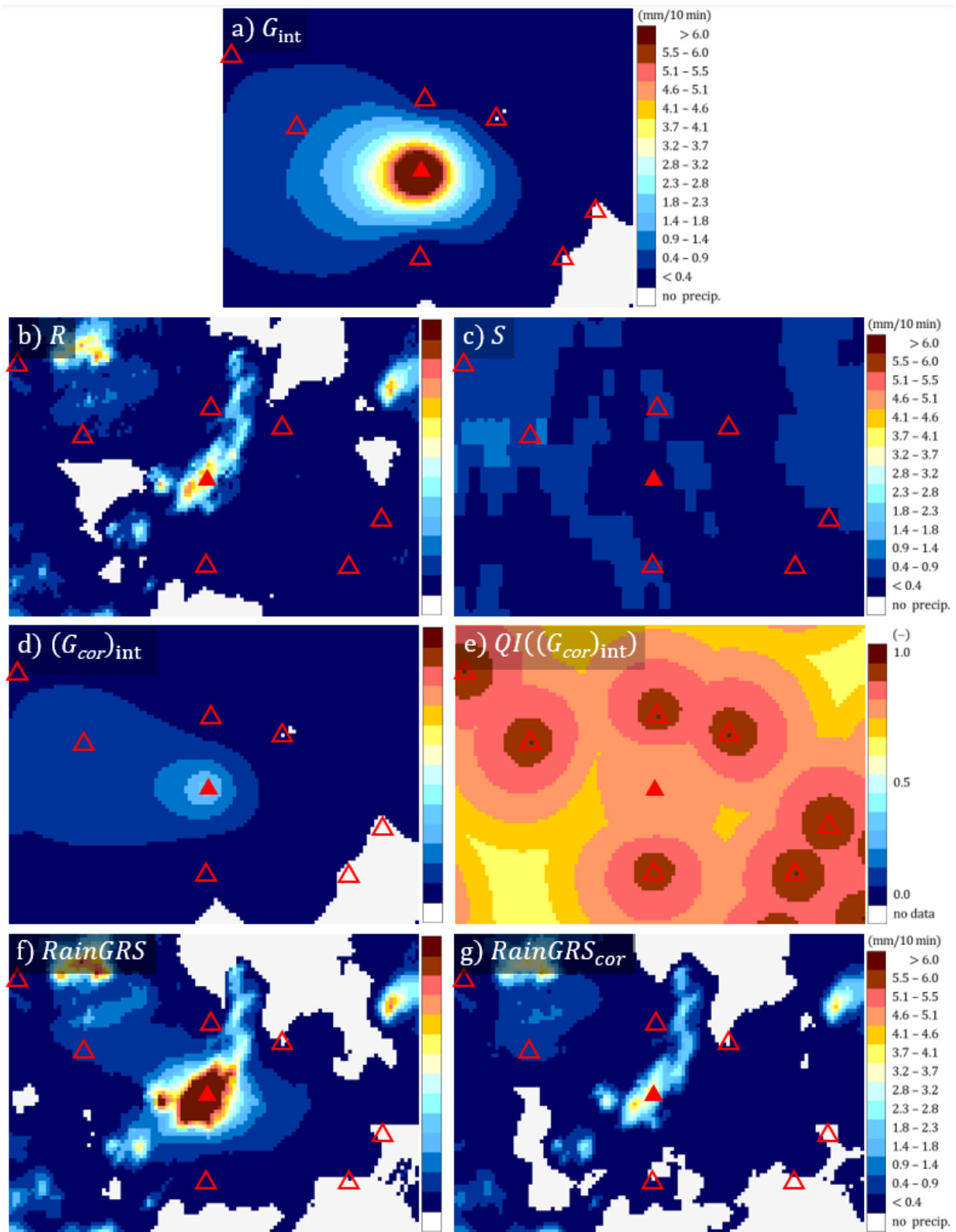
364
365
366
367
368
369
370

Fig. 7d shows the values from individual rain stations after quality control, and Fig. 7e shows the precipitation field after spatial interpolation using the ordinary kriging technique (this field is identical to the one shown in Fig. 6c). As these images show, the precipitation values obtained after data quality control are some mixture of those data from both sensors that passed the QC with higher QI (see section 3.1). The Siercza rain station, marked with a red circle, serves here as an example of a station with incorrect measurement (the original values were 0.2 and 0.0 mm/10 min for unheated and heated sensors, respectively). The erroneous value of 10 mm/10 min was eliminated as a result of the QC algorithms, so the rainfall value for this rain station after QC is 0.2 mm/10 min measured by the unheated sensor.

371 4.3 Example for Nowa Wieś Podgórna rain station from 22 June 2021, 13:30 UTC

372 An example of a rain station with low-quality measurements, taken from the Nowa Wieś Podgórna rain station during June
373 2021, is shown in Fig. 2b (section 2.1). The low quality is evidenced by large differences between the values measured with
374 heated and unheated sensors: the heated sensor recorded much higher 10-minute precipitation accumulations than the unheated
375 one. The data from 22 June 2021, 13:30 UTC are analysed in detail below. The heated sensor of the Nowa Wieś Podgórna rain
376 station reported a very high rainfall of 18.9 mm/10 min, whereas the unheated one reported only 2.7 mm/10 min (Table 2). If
377 QC is not performed, then the heated sensor is generally considered the primary sensor as it operates all year round. The
378 precipitation field resulting from the interpolation of rain gauge data without QC obtained by the ordinary kriging method is
379 shown in Fig. 8a.

380
381



382
383
384
385
386
387
388
389
390

Figure 8: Various fields of 10-minute precipitation accumulation (in mm/10 min) in the vicinity of the Nowa Wieś Podgórna rain station (marked with a red triangle; the locations of other rain stations are marked with empty triangles): a) spatially interpolated field from rain gauge data without QC (G_{int}), b) radar-based precipitation field (R), c) satellite-based precipitation field (S), d) spatially interpolated field from rain gauge data after QC ($(G_{cor})_{int}$), e) QI field for the precipitation field from rain gauge data after QC ($QI((G_{cor})_{int})$), f) multi-source precipitation field ($RainGRS$) obtained from raw rain gauge data, g) multi-source precipitation field ($RainGRS_{cor}$) obtained from rain gauge data after QC. Data from 22 June 2021, 13:30 UTC, fragment from the Polish domain (110 km x 80 km).

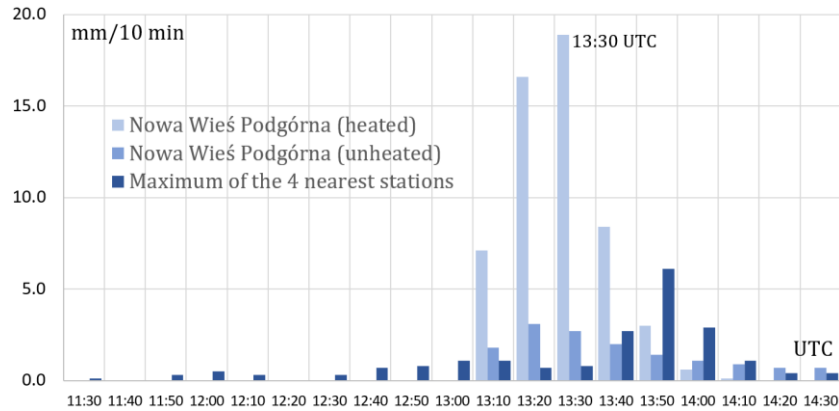
391
392
393
394

In order to diagnose the large difference between the two sensors, a detailed investigation of the situation was performed based on precipitation data from other sources. The radar composite map from the SRI (surface rainfall intensity) product showed 3.95 mm/10 min at this location (Fig. 8b), which is much closer to the value from the unheated sensor. Satellite rainfall, determined from various NWC-SAF products based on Meteosat data (see Section 2.3), showed only 0.05 mm/10 min (Fig.

395 8c); however, measurements based on data from visible and infrared channels are much less accurate than radar measurements.
 396 The radar data confirmed that the rainfall that occurred in the analysed time step in the close vicinity of this rain station is
 397 significantly higher than in the surroundings, but not by as much as the heated sensor reported – it is much closer to the
 398 observation of the unheated sensor.

399 Visually, this conclusion seems to be unquestionable, but it may be interesting how the designed RainGaugeQC scheme
 400 functioned in this situation.

401



402

403 **Figure 9: Precipitation time series at Nowa Wieś Podgórna station in comparison to maximum of four neighbouring rain stations on**
 404 **22 June 2021, from 11:30 to 14:30 UTC.**

405 Fig. 9 shows the recorded precipitation time series from 12 time steps (i.e. two hours) before the analysis date (13:30
 406 UTC), and 6 time steps after this date, at Nowa Wieś Podgórna station (two sensors) and maximum values of the four
 407 neighbouring stations. These stations are located between 19 and 35 km from the analysed Nowa Wieś Podgórna station. Until
 408 the analysis date, precipitation measured by the sensors of these stations was not high, as it was up to about 1 mm/10 min, but
 409 20 min later a significant increase in precipitation of about 6 mm/10 min was observed on both sensors of one of the nearby
 410 stations. At the analysed timestep only Nowa Wieś Podgórna station recorded a slightly higher precipitation on the heated
 411 sensor, while it was drastically higher on the unheated sensor (Table 2).

412

413 **Table 2. Results of QC of the Nowa Wieś Podgórna rain station on 22 June 2021, 13:30 UTC.**

Sensor	G (mm/10 min)	Check				$QI(G)$ (-)
		RC	RSC	TCC	SCC	
Unheated	2.7	Passed	Passed	Failed	Weak outlier	0.75
Heated	18.9	Passed	Passed	Failed	Strong outlier	0.50

414

415 The quality of the data from this rain station was 0.75 for the G_{uh} sensor and 0.50 for G_h . This difference in QI values
 416 was a result of the SCC test, which showed that the G_{uh} sensor differs slightly, and the G_h sensor differs significantly, from the
 417 rainfall values in the neighbouring rain stations within the given subdomain. At the same time, both sensors failed the TCC
 418 test, which in turn indicates that the accumulated values measured by these two sensors over the last 12 time steps differ
 419 significantly (Table 2). This also contributed to a reduction in the final QI value.

420

421 Thus, finally, the value from the unheated sensor G_{uh} is taken for further processing. The precipitation field after the
 422 spatial interpolation of QC data obtained by the ordinary kriging method is shown in Fig. 8d. The precipitation values around
 423 this rain station location are clearly lower than those shown in Fig. 8a (without QC). The QI field for spatially interpolated rain
 424 gauge data is shown in Fig. 8e – the Nowa Wieś Podgórna rain station is of lower quality than the neighbouring rain stations.

424

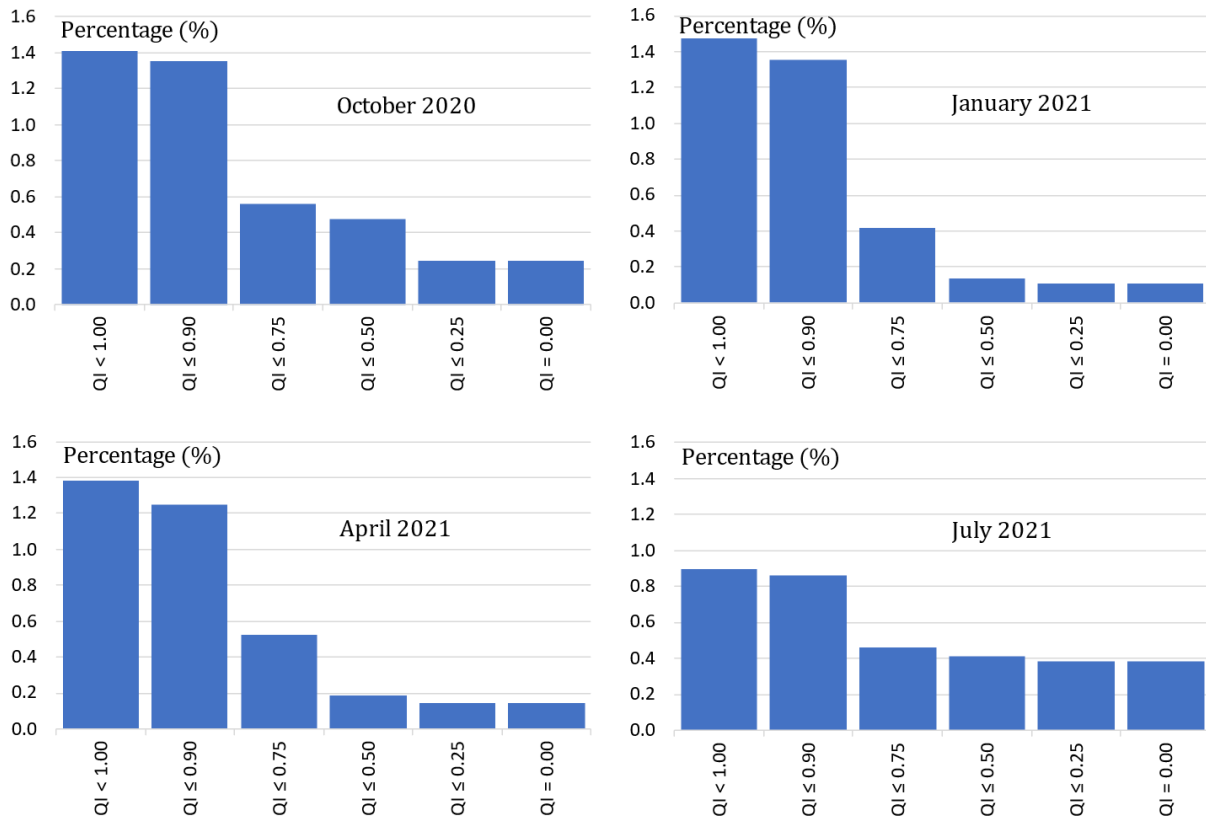
425 QC of rain gauge data influences the precipitation fields produced by applications for the generation of multi-source
 426 fields. This is shown by the example of the QPE fields produced by the RainGRS system, which operationally combines
 precipitation data from rain gauges, weather radar and meteorological satellites (see Section 2.3). In Fig. 8 two fields generated

427 by RainGRS are presented: based on rain gauge data without QC and after QC (Figs. 8f and 8g, respectively). Applying quality
 428 controlled rain gauge data, the RainGRS estimate decreases from 16.19 to 3.26 mm/10 min, which is a very significant effect.

429 4.4 General effects of the operation of the scheme

430 The performance of the RainGaugeQC scheme can be assessed by the degree of QI reduction. This is presented in Fig. 10, for
 431 individual months representative for autumn, winter, spring and summer conditions (October, January, April, and July,
 432 respectively).

433



434

435

436 **Figure 10: Percentage of rain gauge observations with a specified QI reduction after quality control. From top: percentage**
 437 **contribution in each QI interval; cumulative percentage contribution (in %); from left: October 2020, January, April, and July 2021.**

438

The graphs shown do not include the percentage contribution of measurements that were assigned a quality of 1.0; this
 439 is equal to about 98.5–99.1%, much higher than the total contribution of all other values. In general, it can be seen from Fig.
 440 10 that by far the greatest number of reductions in QI values was to values in the range (0.75, 0.90], and this is observed in all
 441 seasons of the year. Relatively large numbers of QI reductions to values in the range (0.50, 0.75] occur in winter (January) and
 442 spring (April), and relatively many data with quality reduced to zero value occur in summer (July) and autumn (October).

443

The number of rain gauge observations with reduced quality is relatively small, below 1.5%. For example, the
 444 contribution of data with QI reduced to zero (i.e. $QI = 0.0$) ranges from about one-third to one-tenth, but grows to about one-
 445 half over the summer (July). In practice, this means that these data were rejected. Probably the most important reason is that
 446 in the summer there often occurs convective precipitation, characterised by high intensities and strong spatial variability, and
 447 moreover rain gauges in no-rain situations react to morning dew condensation, which gives false rainfall measurements
 448 sometimes as high as 0.3 mm/10 min.

449

The most diverse distribution of QI reductions is observed in winter (January): most often there are small decreases in
 450 the QI value. In summer (July), this distribution is the least varied, which can be partially explained by the numerous QI
 451 reductions to zero.

452 5 Conclusions

- 453 1. Quality control of rain gauge data is essential, especially from the perspective of operational applications, when it is
454 not possible to verify gauge data employing highly reliable precipitation measurements, such as manual Hellmann
455 rain gauges, which are not available in real time.
- 456 2. It seems that the RainGaugeQC approach to the QC of rain gauge data, which consists in estimating the value of the
457 *QI* of individual observations, enables more effective use of the data. On the one hand, it is a more cautious approach,
458 as it does not eliminate all suspicious observations, and on the other hand, it enables flexible treatment of any
459 suspected case of data incorrectness.
- 460 3. The IMGW rain station network consists mostly of rain stations equipped with two sensors: unheated and heated.
461 This unique equipment allows the use of pairs of data to conduct much more effective QC. Comparing the
462 observations from two sensors installed at the same location significantly increases the possibility of obtaining
463 information about the uncertainty of measurements, for example by checking the time consistency of the data (TCC
464 check). This is especially important when measurements are carried out with tipping bucket rain gauges, which have
465 relatively low reliability. The availability of observations from both sensors is especially important during the warm
466 season, when convective phenomena prevail. The frequent lack of two sensors installed at the same location reduces
467 the scheme's effectiveness to some extent; however, it remains at a satisfactory level.
- 468 4. It is worth considering the possibility of employing radar data in the RCC and SCC algorithms to detect erroneous
469 rain gauge measurements and to assess their reliability, based on the difference between the values from rain gauge
470 and weather radar. The case study proved that the RainGaugeQC system can identify regionally inconsistent data
471 thanks to the use of radar data as well as neighbouring rain gauge data.
- 472 5. The presented set of algorithms is based on empirical relationships that are strongly dependent on local conditions,
473 both technical and geographic. The most important factors are the density of the rain station network, the availability
474 of other data that can be used as a reference for QC (e.g. from the weather radar network), the type of sensors (their
475 failure rate and measurement uncertainty), as well as terrain orography, wind conditions, and surface precipitation
476 type. Therefore, any changes in the network configuration necessitate recalibration of the algorithms.
- 477 6. The number of rain gauge observations with reduced *QI* following QC under the RainGaugeQC scheme is relatively
478 small, as it is below 1.5%. In all seasons, the highest number of *QI* value reductions was to values in the range [0.75,
479 0.90). The highest number of erroneous data (with *QI* reduced to zero) is found in summer (July) (approximately
480 0.4%), whereas in other seasons it ranges from about 0.10% to 0.23%.

481 Appendix 1. Detailed description of the Radar Conformity Check (RCC) algorithm

482 RCC is performed to identify false zero precipitation and false gauge-reported precipitation measurement by applying radar
483 data.

- 484 1. Identifying false zero precipitation.
485 Each gauge sensor value (*G*) less than 0.2 mm/10 min is checked against radar observations (*R*) at the gauge location
486 and in its vicinity within a grid of 3 pixels x 3 pixels.
487 If at least one pixel of radar data had precipitation above 0.4 mm/10 min, then the gauge value measured by
488 this sensor is assumed to be erroneous, thus the sensor value is replaced by “no data” and the quality of this sensor
489 is reduced to 0.
- 490 2. Identifying false gauge-reported precipitation.
491 Each gauge sensor value (*G*) above 0 mm/10 min is checked against radar observations (*R*) at the gauge location and
492 in its vicinity within a grid of 3 pixels x 3 pixels.

493 If at least two radar pixels with $QI > 0.85$ returned “no precipitation” ($R = 0$ mm/10 min), then the following
494 conditions are checked:

- 495 (a) If for a given rain station, data are available only from one sensor (G) and $G > 0$ mm/10 min, then:
- 496 – if the station is located in a mountain or foothill area, the sensor is considered erroneous and its value is
497 replaced by $G = 0$ mm and its quality reduced by 0.5;
 - 498 – if the station is located in a lowland area, the sensor is considered erroneous and its value is replaced by
499 $G = 0$ mm and its quality reduced by 0.25.
- 500 (b) If for a given rain station, data are available from two sensors (heated G_h and unheated G_{uh}) and $G_h > 0$ mm/10
501 min and $G_{uh} > 0$ mm/10 min, then:
- 502 – if the station is located in a mountain or foothill area and values from both sensors are similar, i.e. SF
503 (G_{uh}, G_h) = “true”, then the quality of both sensors is reduced by 0.75, but if SF (G_{uh}, G_h) = “false” then
504 their qualities are reduced to $QI = 0$ and the sensor values are replaced by “no data”;
 - 505 – if the station is located in a lowland area, then the sensor qualities are reduced to $QI = 0$ and the sensor
506 values are replaced by “no data”.
- 507 (c) If for a given rain station, data are available from two sensors (heated G_h and unheated G_{uh}) and one of them
508 reports “no precipitation” (i.e. $G_h = 0$ mm/10 min or $G_{uh} = 0$ mm/10 min), then:
- 509 – if the rain station is located in a mountain or foothill area and the values from both sensors are similar
510 (i.e. SF (G_{uh}, G_h) = “true”), then the QI of the sensor which observed precipitation $G > 0$ mm/10 min is
511 reduced by 0.75, but if SF (G_{uh}, G_h) = “false”, then the QI of the sensor which reports $G > 0$ mm/10 min
512 is reduced to $QI = 0$ and the sensor value is replaced by “no data”;
 - 513 – if the rain station is located in a lowland area, then the quality of the sensor that reports $G > 0$ mm/10 min
514 is reduced to $QI = 0$ and the sensor value is replaced by “no data”.

515 Appendix 2. Detailed description of the Temporal Conformity Check (TCC) algorithm

516 The first step of this check is performed to detect constant values observed by a given sensor. If the same value (e.g. 0.1 mm/10
517 min) is reported for a certain number of time steps (e.g. nine consecutive observations), then the sensor is probably clogged.
518 In this case, the blocked sensor has failed the TCC test, its QI is reduced to 0, and the TCC test cannot be performed for the
519 other sensor.

520 The main part of TCC serves to identify rain stations for which there are large differences between values measured
521 simultaneously by pairs of rain sensors (G_h, G_{uh}), which may be evidence of their low quality. This check requires
522 measurements from both rain gauge sensors at the same location; it can thus be conducted only in the warm season, when both
523 sensors provide measurements. This lasts from April to October, when data from unheated sensors (G_{uh}) are available; the
524 heated sensors (G_h) operate all year round.

- 525 1. Pairs of simultaneous measurements from two sensors are verified for the last 12 time steps, excluding observations
526 of poor quality (which QI is 0.0 for previous time steps and for the current time step failed GEC, RC, or RCC check).
527 If the number of the pairs is high enough (at least 9), the cumulative sums are calculated:

$$528 \quad S_h = \sum_{i=1}^n G_{h,i}, \quad S_{uh} = \sum_{i=1}^n G_{uh,i} \quad (5)$$

- 529 2. The similarity of the accumulated sums is checked by means of the SF function. If they differ significantly, i.e. if
530 $SF(S_h, S_{uh}) = \text{“false”}$, then the data from both sensors have failed the TCC test and their quality is reduced by 0.25.

531 **Appendix 3. Detailed description of the Spatial Consistency Check (SCC) algorithm**

532 The SCC procedure consists of the following steps:

- 533 1. The Polish domain (900 km x 800 km) is divided into subdomains with dimensions of 100 km x 100 km. Only data
534 with $QI > 0$ after previous tests are subject to this check. It is optional: (i) to analyse both sensors, heated and
535 unheated, together or separately, (ii) to include also data from the previous time step (10 min ago) if their $QI = 1.0$.
536 In order to perform this check there must be data available from at least three stations in a subdomain; otherwise
537 the test is not performed for that subdomain.
- 538 2. Based on data from rain stations (G) located in a given subdomain, the following percentiles are determined: 25%,
539 50% (median), and 75% ($Q_{25}(G)$, $Q_{med}(G)$, and $Q_{75}(G)$, respectively).

540 The median absolute deviation (MAD) for a given subdomain is determined from the formula:

$$541 \quad MAD = \frac{1}{n} \sum_{i=1}^n |G_i - Q_{med}(G)| \quad (6)$$

542 where n is the number of data, G_i is the i -th sensor value, and $Q_{med}(G)$ is the median.

- 543 3. The index D_i , which determines numerically the deviation of the precipitation value measured with the i -th sensor
544 from the median of all sensors within a given subdomain, is calculated from the formula (Kondragunta and
545 Shrestha, 2006):

$$546 \quad D_i = \begin{cases} 0 & MAD = 0 \\ \frac{|G_i - Q_{med}(G)|}{MAD} & MAD \neq 0 \text{ and } Q_{75}(G) = Q_{25}(G) \\ \frac{|G_i - Q_{med}(G)|}{Q_{75}(G) - Q_{25}(G)} & MAD \neq 0 \text{ and } Q_{75}(G) \neq Q_{25}(G) \end{cases} \quad (7)$$

547 Following calculation of the D_i values for all sensors within a given subdomain, three percentiles are
548 determined: 90%, 95%, and 99% ($Q_{90}(D)$, $Q_{95}(D)$, and $Q_{99}(D)$, respectively).

- 549 4. If $D_i \leq Q_{90}(D)$, then the i -th sensor is not an outlier and the test is passed.

550 If this is not the case, the i -th sensor is flagged and the formula (8) is applied to compare the index D_i with
551 the three percentile values, in order to determine to which class of outliers the given value belongs:

$$552 \quad \text{outlier} = \begin{cases} \text{strong} & D_i > Q_{99}(D) \\ \text{medium} & Q_{95}(D) < D_i \leq Q_{99}(D) \\ \text{weak} & Q_{90}(D) < D_i \leq Q_{95}(D) \end{cases} \quad (8)$$

553 The procedure is repeated in four subdomains resulting from shifting the given subdomain vertically (west-
554 east) and horizontally (south-north), i.e. in four directions, with offsets of 25 km (except for subdomains on the
555 edges and corners of the domain, which are shifted in three and two directions, respectively). If the value measured
556 with a given sensor is flagged in all analysed subdomains, it fails the SCC check. If the values belonged to different
557 classes of outliers, the weakest one is assigned to the sensor for further processing.

- 558 5. For sensors that failed the SCC check, if the data from both sensors are available for a given rain station and they
559 are similar, i.e. $SF(G_h, G_{uh}) = \text{"true"}$, and passed the TCC check, then the QI for the sensor is not reduced.

560 Otherwise, each outlier is verified against radar data. For this purpose the following values are determined
561 within a grid of 5 pixels x 5 pixels around this rain station location: $\min(QI(R))$ – the minimum quality QI of the
562 radar precipitation R ; $R_{max} = \max(R: QI(R) > 0.75)$ – the maximum value of radar precipitation with a quality
563 above 0.75; $QI(R_{max})$ – the quality of the maximum value of radar precipitation R_{max} . This verification algorithm
564 is as follows:

565 If $\min(QI(R)) > 0.75$, then: (9)

566 if $R_{max} = 0$, then the quality is reduced by 1.0 and $G = \text{"no data"}$;

567 if ($G > 1.0 \text{ mm}$) and $\left(\frac{G}{R_{max}} < \frac{QI(R_{max})}{4.0} \text{ or } \frac{G}{R_{max}} > \frac{4.0}{QI(R_{max})}\right)$, then:

568
$$QI = \begin{cases} QI - 1.00 & \text{strong outlier} \\ QI - 0.50 & \text{medium outlier} \\ QI - 0.20 & \text{weak outlier} \end{cases}$$

569 if ($G > 1.0 \text{ mm}$) and $\left(\frac{G}{R_{max}} \geq \frac{QI(R_{max})}{4.0} \text{ and } \frac{G}{R_{max}} \leq \frac{4.0}{QI(R_{max})}\right)$, then:

570
$$QI = \begin{cases} QI - 0.25 & \text{strong outlier} \\ QI - 0.10 & \text{medium outlier} \\ QI & \text{weak outlier} \end{cases}$$

571 If ($G \leq 1.0 \text{ mm}$) or ($\min(QI(R)) \leq 0.75$), then:

572
$$QI = \begin{cases} QI - 0.25 & \text{strong outlier} \\ QI - 0.10 & \text{medium outlier} \\ QI & \text{weak outlier} \end{cases}$$

573 where $\frac{4.0}{QI(R_{max})}$ is the limitation to the magnitude of disparity $\frac{G}{R_{max}}$ determined empirically.

574 An alternative simplified analysis of the spatial consistency of rain gauge data may be performed analogously to steps
575 1–4, especially if radar data are unavailable. In this case, it is sufficient to determine only the $Q_{95}(D)$ percentile. Here, if in all
576 subdomains $D_i > Q_{95}(D)$, the sensor fails the SCC, and the QI is decreased by 0.10.

577

578 *Code availability.* The rain gauge data are processed by the RainGaugeQC software developed at the IMGW, which owns the
579 economic property rights to the software.

580

581 *Data availability.* The work described in this article is focused on general processing of rain gauge data to improve their
582 quality, not concentrating on a specific data set, thus data have not been attached. Rain gauge data are collected in the IMGW
583 database.

584

585 *Author contributions.* KO, IO, and JS designed algorithms of the RainGaugeQC system. KO developed the software code and
586 performed the simulations. JS, IO, and KO prepared the manuscript. JS made figures.

587

588 *Competing interests.* The authors declare that they have no conflict of interest.

589 **References**

590 Baserud, L., Lussana, C., Nipen, T.N., Seierstad, I.A., Oram, L., and Aspelien, T.: TITAN automatic spatial quality control of
591 meteorological in-situ observations, *Advances in Science and Research*, 17, 153-163, [https://doi.org/10.5194/asr-17-](https://doi.org/10.5194/asr-17-153-2020)
592 153-2020, 2020.

593 Bárdossy, A., Seidel, J., and El Hachem, A.: The use of personal weather station observation for improving precipitation
594 estimation and interpolation, *Hydrology and Earth System Sciences*, 25, 583–601, [https://doi.org/10.5194/hess-25-583-](https://doi.org/10.5194/hess-25-583-2021)
595 2021, 2021.

596 Blenkinsop, S., Lewis, E., Chan, S.C., and Fowler, H.J.: An hourly precipitation dataset and climatology of extremes for the
597 UK. *International Journal of Climatology*, 37, 722–740, doi.org/10.1002/joc.4735, 2017.

598 Buisán, S. T., Earle, M. E., Collado, J. L., Kochendorfer, J., Alastrué, J., Wolff, M., Smith, C. D., and López-Moreno, J. I.:
599 Assessment of snowfall accumulation underestimation by tipping bucket gauges in the Spanish operational network,
600 Atmospheric Measurement Techniques, 10, 1079–1091, <https://doi.org/10.5194/amt-10-1079-2017>, 2017.

601 Burszta-Adamiak, E., Licznar, P., and Zaleski, J.: Criteria for identifying maximum rainfall determined by the peaks-over-
602 threshold (POT) method under the Polish Atlas of Rainfall Intensities (PANDa) project, Meteorology Hydrology and
603 Water Management, 7, 3-13, <https://doi.org/10.26491/mhwm/93595>, 2019.

604 Colli, M., Lanza, L.G., and La Barbera P.: Performance of a weighing rain gauge under laboratory simulated time-varying
605 reference rainfall rates, Atmospheric Research, 131, 3-12, <https://doi.org/10.1016/j.atmosres.2013.04.006>, 2013.

606 de Vos, L. W., Leijnse, H., Overeem, A., and Uijlenhoet, R.: Quality control for crowdsourced personal weather stations to
607 enable operational rainfall monitoring, Geophysical Research Letters, 46, 8820–8829,
608 <https://doi.org/10.1029/2019GL083731>, 2019.

609 Einfalt, T., Szturc, J., and Ośródk, K.: The quality index for radar precipitation data – a tower of Babel? Atmos. Sci. Lett.,
610 11, 139-144. <https://doi.org/10.1002/asl.271>, 2010.

611 Fiebrich, C. A., Morgan, C. R., and McCombs, A. G.: Quality assurance procedures for mesoscale meteorological data. Journal
612 of Atmospheric and Oceanic Technology, 27, 1565–1582, <https://doi.org/10.1175/2010JTECHA1433.1>, 2010.

613 Førland, E. J., Allerup, P., Dahlstrom, B., Elomaa, E., Jonsson, T., Madsen, H., Perala, H., Rissanen, P., Vedin, H., and Vejen,
614 F.: Manual for operational correction of Nordic precipitation data. Report Nr 24/96. DNMI, Norway, pp. 66, 1996.

615 Golz, C., Einfalt, T., Gabella, M., and Germann, U.: Quality control algorithms for rainfall measurements, Atmospheric
616 Research, 77, 247-255, <https://doi.org/10.1016/j.atmosres.2004.10.027>, 2005.

617 Goodison, B.E., Louie, P.Y.T., and Yang, D.: WMO solid precipitation measurement intercomparison: Final report, Instrum.
618 Obs. Methods Rep. 67, World Meteorological Organization, Geneva, Switzerland. pp. 211, 1998.

619 Grossi, G., Lendvai, A., Giovanni Peretti, G., and Ranzi, R.: Snow precipitation measured by gauges: systematic error
620 estimation and data series correction in the Central Italian Alps. Water, 9, 461, <https://doi.org/10.3390/w9070461>, 2017.

621 Habib, E., Krajewski, W., and Kruger, A.: Sampling errors of tipping-bucket rain gauge measurements, Journal of Hydrologic
622 Engineering, 6, 159-166, [https://doi.org/10.1061/\(ASCE\)1084-0699\(2001\)6:2\(159\)](https://doi.org/10.1061/(ASCE)1084-0699(2001)6:2(159)), 2001.

623 Jurczyk, A., Szturc, J., Otop, I., Ośródk, K., and Struzik, P.: Quality-based combination of multi-source precipitation data,
624 Remote Sensing, 12, 1709, <https://doi.org/10.3390/rs12111709>, 2020.

625 Kochendorfer, J., Earle, M. E., Hodyss, D., Reverdin, A., Roulet, Y.-A., Nitu, R., Rasmussen, R., Landolt, S., Buisan, S., and
626 Laine, T.: Undercatch adjustments for tipping-bucket gauge measurements of solid precipitation, Journal of
627 Hydrometeorology, 21, 1193–1205, <https://doi.org/10.1175/JHM-D-19-0256.1>, 2020.

628 Kondragunta, C. R. and Shrestha, K.: Automated real-time operational rain gauge quality-control tools in NWS Hydrologic
629 Operations. 86th AMS Annual Meeting, Atlanta, GA, 28 January – 3 March 2006, 2006.

630 Lewis, E., Quinn, N., Blenkinsop, S., Fowler, H. J., Freer, J., Tanguy, M., Hitt, O., Coxon, G., Bates, P., and Woods, R.: A
631 rule based quality control method for hourly rainfall data and a 1 km resolution gridded hourly rainfall dataset for Great
632 Britain: CEH-GEAR1hr, Journal of Hydrology, 564, 930-943, <https://doi.org/10.1016/j.jhydrol.2018.07.034>, 2018.

633 Lewis, E., Pritchard, D., Villalobos-Herrera, R., Blenkinsop, S., McClean, F., Guerreiro, S., Schneider, U., Becker, A., Finger,
634 P., Meyer-Christoffer, A., Rustemeier, E., and Fowler, H. J.: Quality control of a global hourly rainfall dataset,
635 Environmental Modelling & Software, 144, 105169, <https://doi.org/10.1016/j.envsoft.2021.105169>, 2021.

636 Martinaitis, S. M., Cocks, S. B., Qi, B., Kaney, Y., Zhang, J., and Howard, K.: Understanding winter precipitation impacts on
637 automated gauges within a real-time system, Journal of Hydrometeorology, 16, 2345-2363,
638 <https://doi.org/10.1175/JHM-D-15-0020.1>, 2015.

639 Michelson, D.: Systematic correction of precipitation gauge observations using analyzed meteorological variables, Journal of
640 Hydrology, 290, 161–177, <https://doi.org/10.1016/j.jhydrol.2003.10.005>, 2004.

641 Moslemi, M. and Joksimovic, D.: Real-time quality control and infilling of precipitation data using neural networks, EPiC
642 Series in Engineering (HIC 2018. 13th International Conference on Hydroinformatics), 3, 1457-1464,
643 <https://doi.org/10.29007/t5k7>, 2018.

644 Neuper, M. and Ehret, U.: Quantitative precipitation estimation with weather radar using a data- and information-based
645 approach, *Hydrology and Earth System Sciences*, 23, 3711–3733, <https://doi.org/10.5194/hess-23-3711-2019>, 2019.

646 Niu, G., Yang, P., Zheng, Y., Cai, X., and Qin, H.: Automatic quality control of crowdsourced rainfall data with multiple
647 noises: A machine learning approach, *Water Resources Research*, 57, e2020WR029121,
648 <https://doi.org/10.1029/2020WR029121>, 2021.

649 Ośródką, K., Szturc, J., and Jurczyk A.: Chain of data quality algorithms for 3-D single-polarization radar reflectivity
650 (RADVOL-QC system), *Meteorological Applications*, 21, 256-270, <https://doi.org/10.1002/met.1323>, 2014.

651 Ośródką, K. and Szturc, J.: Improvement in algorithms for quality control of weather radar data (RADVOL-QC system),
652 *Atmospheric Measurement Techniques*, 15, 261-277, <https://10.5194/amt-15-261-2022>, 2022.

653 Otop, I., Szturc, J., Ośródką, K. and Djaków, P.: Automatic quality control of telemetric rain gauge data for operational
654 applications at IMGW-PIB, *ITM Web Conf.*, 23, 00028, <https://doi.org/10.1051/itmconf/20182300028>, 2018.

655 Qi, Y., Martinaitis, S., Zhang, J., and Cocks, S.: A real-time automated quality control of hourly rain gauge data based on
656 multiple sensors in MRMS System, *Journal of Hydrometeorology*, 17, 1675-1691, <https://doi.org/10.1175/JHM-D-15-0188.1>, 2016.

657

658 Rasmussen, R., Baker, B., Kochendorfer, J., Meyers, T., Landolt, S., Fischer, A. P., Black, J., Theriault, J. M., Kucera, P.,
659 Gochis, D., Smith, C., Nitu, R., Hall, M., Ikeda, K., and Gutmann, E.: How well are we measuring snow? The
660 NOAA/FAA/NCAR winter precipitation Test Bed, *Bulletin of the American Meteorological Society*, 93, 811-829,
661 <https://doi.org/10.1175/BAMS-D-11-00052.1>, 2012.

662 Savina, M., Schappi, B., Molnar, P., Burlando, P., and Sevruk, B.: Comparison of a tipping-bucket and electronic weighing
663 precipitation gauge for snowfall, *Atmospheric Research*, 103, 54-51, <https://doi.org/10.1016/j.atmosres.2011.06.010>,
664 2012.

665 Scherrer, S. C., Frei, C., Croci-Maspoli, M., van Geijtenbeek, D., Hotz, C., and Appenzeller C.: Operational quality control of
666 daily precipitation using spatio-climatological plausibility testing, *Meteorologische Zeitschrift*, 20, 397-407,
667 <https://doi.org/10.1127/0941-2948/2011/0236>, 2011.

668 Sevruk, B.: Adjustment of tipping-bucket precipitation gauge measurements, *Atmospheric Research*, 42, 237-246,
669 [https://doi.org/10.1016/0169-8095\(95\)00066-6](https://doi.org/10.1016/0169-8095(95)00066-6), 1996.

670 Sevruk, B. and Nevenic, M.: The geography and topography effects on the areal pattern of precipitation in a small prealpine
671 basin, *Water Science and Technology*, 37, 163-170, 1998.

672 Sevruk, B., Ondras M., and Chvila B.: The WMO precipitation intercomparisons, *Atmospheric Research*, 92, 376-380,
673 <https://doi.org/10.1016/j.atmosres.2009.01.016>, 2009.

674 Shedekar, V. S., King, K. W., Fausey, N. R., Soboyejo, A. B. O., Harmel, R. D., and Brown, L. C.: Assessment of measurement
675 errors and dynamic calibration methods for three different tipping bucket rain gauges, *Atmospheric Research*, 178, 445-
676 458, <https://doi.org/10.1016/j.atmosres.2016.04.016>, 2016.

677 Sieck, L.C., Burges, S. J. and Steiner, M.: Challenges in obtaining reliable measurements of point rainfall, *Water Resources*
678 *Research*, 43, W01420, <https://doi.org/10.1029/2005WR004519>, 2007.

679 Steinacker, R., Mayer, D., Steiner, A.: Data quality control based on self-consistency, *Monthly Weather Review*, 139, 3974–
680 3991, <https://doi.org/10.1175/MWR-D-10-05024.1>, 2011.

681 Szturc, J., Jurczyk, A., Ośródką, K., Wyszogrodzki, A., and Giszterowicz, M.: Precipitation estimation and nowcasting at
682 IMGW (SEiNO system), *Meteorology Hydrology and Water Management*, 6, 3–12,
683 <https://doi.org/10.26491/mhwm/76120>, 2018.

684 Szturc, J., Ośródk, K., Jurczyk, A., Otop, I., Linkowska, J., Bochenek, B., and Pasierb, M.: Quality control and verification
685 of precipitation observations, estimates, and forecasts, in: *Precipitation Science. Measurement, Remote Sensing,*
686 *Microphysics and Modeling*, Michaelides, S., edited by: Elsevier 2022, 91-133, [https://doi.org/10.1016/B978-0-12-](https://doi.org/10.1016/B978-0-12-822973-6.00002-0)
687 [822973-6.00002-0](https://doi.org/10.1016/B978-0-12-822973-6.00002-0), 2022.

688 Taylor, J. R. and Loescher, H. L.: Automated quality control methods for sensor data: a novel observatory approach,
689 *Biogeosciences*, 10, 4957-4971, <https://doi.org/10.5194/bg-10-4957-2013>, 2013.

690 Upton, G. and Rahimi A.: On-line detection of errors in tipping-bucket raingauges, *Journal of Hydrology*, 278, 197-212,
691 [https://doi.org/10.1016/S0022-1694\(03\)00142-2](https://doi.org/10.1016/S0022-1694(03)00142-2), 2003.

692 Urban, G. and Strug, K.: Evaluation of precipitation measurements obtained from different types of rain gauges,
693 *Meteorologische Zeitschrift*, 30, 445-463, <https://doi.org/10.1127/metz/2021/1084>, 2021.

694 Villalobos Herrera, R., Blenkinsop, S., Guerreiro, S. B., O'Hara, T., Fowler, H. J.: Sub-hourly resolution quality control of
695 rain gauge data significantly improves regional sub-daily return level estimates, *Quarterly Journal of the Royal*
696 *Meteorological Society* (accepted author manuscript), <https://doi.org/10.1002/qj.4357>, 2022.

697 WMO-No. 8: Guide to Instruments and Methods of Observation, vol. I: Measurement of Meteorological Variables, 2018
698 edition. World Meteorological Organization, Geneva, pp. 548., 2018.

699 WMO-No. 305: Guide on the Global Data-processing System, 1993 edition. World Meteorological Organization, Geneva, pp.
700 199, 1993.

701 WMO-No. 488: Guide to the Global Observing System, 2010 edition, updated in 2017. World Meteorological Organization,
702 Geneva, pp. 215, 2017.

703 Yeung, H. Y., Man, C., Chan S. T., and Seed, A.: Development of an operational rainfall data quality-control scheme based
704 on radar-raingauge co-kriging analysis, *Hydrological Sciences Journal*, 59, 1293-1307,
705 <https://doi.org/10.1080/02626667.2013.839873>, 2014.

706 You, J., Hubbard K. G., Nadarajah S., and Kunkel K. E.: Performance of quality assurance procedures on daily precipitation,
707 *Journal of Atmospheric and Oceanic Technology*, 24, 821-834, <https://doi.org/10.1175/JTECH2002.1>, 2007.

708